Z. Phys. B - Condensed Matter 53, 1-13 (1983)

Condensed
Zeitschrift für Physik B Matter

The Scaling Theory of Electrons in Disordered Solids: Additional Numerical Results

A. MacKinnon
The Blackett Laboratory, Imperial College, London, England

B. Kramer
Physikalisch-Technische Bundesanstalt, Braunschweig, Federal Republic of Germany

Received July 25, 1983

We present extensive numerical results applying the finite size scaling method to the theory of electrons in disordered systems. A method is developed for studying the localisation length in 1-dimensional systems of finite cross section. By studying these results as a function of cross-section and using scaling ideas, we derive the critical properties of 2-D and 3-D systems. We calculate transport properties as a function of temperature which can then be compared with experiment.

1. Introduction

In recent years, since the formulation of the scaling hypothesis for localisation by Abrahams et al. [1] the subject of Anderson localisation has attracted increasing interest with a rapid development of new theoretical and experimental approaches. Diagrammatic expansion of the conductivity proved particularly useful in the regime of *weak impurity scattering*, and led to the most spectacular result that all states in the two dimensional ($2d$) disordered system should be localised in the thermodynamic limit giving rise to logarithmic effects in the conductance as a function of the various parameters, such as the temperature, the frequency and the system size [1-3]. One of the most important experimental results was the discovery of the logarithmic increase of the resistance of ultrathin metallic films and inversion layers with decreasing temperature [4-7]. This, together with the theoretical prediction that interaction effects should result in a similar behaviour [8, 9], showed that the effects of the disorder and particle-particle interactions are much more subtle than assumed hitherto, especially if combined with an external magnetic field [10], and the peculiarities of the band structure in semiconductors [11]. Questions like whether the electronic states contributing to the transport are truly exponentially localised or power law localised are still controversial [12]. On the other hand, the regime of *strong scattering* in three dimensions ($3d$) where the scaling theory yields an Anderson transition at a finite disorder while seemingly quantitatively understood [13] still offers such basic questions as to what extent quantum mechanical effects are important for the transition, and the precise critical behaviour of the localisation length and the conductivity.

At about the same time serious doubts began to emerge about the reliability of the numerical methods, which had been applied to the problem [14]. Attempts to calculate the dc-conductivity of a disordered one dimensional ($1d$) system directly from the Kubo-Greenwood formula failed to confirm the absence of diffusion for all values of the disorder parameter, however small [15]. The resolution of this contradiction helped however to clarify the conditions affecting the conclusiveness of numerical results [16-19]. The finite system sizes used (about 10,000 lattice constants) were not sufficient to prevent large fluctuations depending on whether the Fermi energy lay between eigenenergies or exactly at one. The standard way around this problem in volved the introduction of a broadening of the energy levels, which implied in some sense inelastic scattering. This then dominated the behaviour of the conductivity for low disorder.

It was therefore clear that the size of the systems studied had to be substantially increased to over-

come these problems [19]. Since the restriction on the system size was due to the size of the computer's core store it was necessary to find a method which does not suffer in this way. One possibility is to approach the thermodynamic limit by implementing directly the renormalisation group idea, i.e. constructing successively larger systems from ensembles of comparatively small subsystems [20–22]. Although system sizes could be increased by one order of magnitude in $2d$ using this technique the method still suffered from the same problems as described above. Consequently, the results seemed to be inconsistent with the scaling hypothesis mentioned at the beginning [21]. Another possibility arises from the study of one dimensional disordered systems [23–26]. The idea is to embed the system in an infinite ideal metal, which serves to generate a continuous energy spectrum, and which can be treated analytically [27].

The Anderson Hamiltonian [28] may be written in the form

$$H=\sum_i \varepsilon_i |i\rangle\langle i| + V\sum_{ij} |i\rangle\langle j| \tag{1}$$

where the diagonal elements ε_i are independent random variables and j is summed over the nearest neighbors of i. The off-diagonal element V is constant and the units may be chosen so that $V=1$. The corresponding Schrödinger equation for $1d$ may be written as

$$a_{i+1}=(E-\varepsilon_i)a_i - a_{i-1} \tag{2}$$

which provides us with a recursion formula for the coefficients a_i of the wave function. This rises exponentially with probability one with increasing i for all non-zero values of the width of the distribution of the ε_i. The computer storage needed to implement this formula is independent of the length of the chain as required to fulfil the conditions discussed above.

This paper is devoted to the results of a generalisation of this method. In Sect. 2, the method for $1d$ is widened to systems of finite cross section. In Sect. 3 the results of the scaling theory and its application to such systems are discussed. Similar ideas have been used before in quantum Hamiltonian field theory [29] and the theory of spin glasses [30] making use of a refinement of phenomenological renormalisation [31–32]. Finally, in Sect. 4 the transport properties of systems at finite temperature are derived from finite size scaling arguments.

2. Methods for Systems with Finite Cross Section

In this section we discuss the technical details of the generalisation of the method for $1d$ systems sketched in the introduction to systems of finite cross section. Since we started our work there has been some progress in the study of the analytical properties of such systems [33–35]. Several points which where previously little more than plausible assumptions have since been rigorously proven.

There are two closely related methods of calculating the localisation length on such a system, the Green's Function method [36], and the Transfer Matrix method [37]. Both methods attempt to solve the generalised form of (2)

$$A_{n+1}=(E-H_n)A_n - A_{n-1}. \tag{3}$$

The energy units have again been defined so that the (constant) off-diagonal elements of the Hamiltonian are unity. H_n is the Hamiltonian of the n^{th} $(d-1)$ dimensional slice of the d dimensional "bar" when it is not coupled to the rest. All quantities in (3) are matrices operating in a $(d-1)$ dimensional subspace.

a) Green's Function Method

First let us define the localisation length λ on the "bar" by

$$\frac{2}{\lambda} = -\lim_{n\to\infty}\frac{1}{n}\ln \mathrm{Tr}|G_{1n}|^2 \tag{4}$$

where G_{1n} is the submatrix of the Green's function or resolvent coupling pairs of atoms at opposite ends of a "bar" of length n. G_{1n} can be found by iterating the equations

$$G_{1n+1}=G_{1n}G_{n+1n+1}, \tag{5a}$$

$$G_{n+1n+1}=[E-H_{n+1}-G_{nn}]^{-1}. \tag{5b}$$

Equations (3) and (5) are related by

$$A_{n+1}=G_{1n}^{-1}, \tag{6a}$$

$$A_1=\mathbf{1}, \tag{6b}$$

$$A_0=0 \tag{6c}$$

which may be verified by insertion.

Iteration of (5) is computationally more complicated that (3) since the former involves a matrix inversion at each stage. The eigenvalues of A_n however rise exponentially with the length of the "bar" such that when the ratio of the smallest to the largest eigenvalue becomes comparable with the machine ac-

curacy the smallest is lost. It is however this smallest eigenvalue of A_n, which provides the dominant contribution to G_{1n} and therefore to λ

This difficulty may be removed by the following transformation, which has to be performed regularly (e.g. every 10^{th} step) but not necessarily at each step.

$$\bar{A}_n = \mathbf{1}, \tag{7a}$$

$$\bar{A}_{n-1} = A_{n-1} A_n^{-1} \tag{7b}$$

which implies via (3)

$$\bar{A}_{n+1} = A_{n+1} A_n^{-1}. \tag{7c}$$

Further, we define

$$\bar{B}_n = B_{n-1} A_n^{-1} / b_n \tag{7d}$$

where

$$b_n^2 = \sum_{ij} |(B_{n-1} A_n^{-1})_{ij}|^2 \equiv \|B_{n-1} A_n^{-1}\|^2 \tag{8}$$

and with $B_0 = \mathbf{1}$ at the beginning.

Thus, while the iteration of (3) starts again from initial values of the order unity, after another step

$$\begin{aligned} b_{n+1}^2 &= \|\bar{B}_n \bar{A}_{n+1}^{-1}\|^2 \\ &= \|A_{n+1}^{-1}\|^2 / b_n^2 \\ &= \mathrm{Tr}\,|G_{1n}|^2 / b_n^2 \end{aligned} \tag{9}$$

still contains the full information about the resolvent between the first and the n^{th} slice of the system. The localisation length may then be calculated iteratively as follows

$$\lambda_n = -\frac{n}{c_n} \tag{10}$$

where

$$c_n = c_{n-1} + \ln b_n \tag{11}$$

and $c_0 = 0$ at the beginning.

Correspondingly, the statistical error in λ_n may be calculated from

$$\Delta_n^2 = \frac{d_n}{n} - \left(\frac{c_n}{n}\right)^2 \tag{12}$$

where

$$d_n = d_{n-1} + (\ln b_n)^2 \tag{13}$$

and $d_0 = 0$.

Δ was used to decide whether λ_n had converged. In agreement with earlier work [38, 39] for $1d$ systems it was found that the length of the "bar" required for convergence is proportional to λ and is approximately given by

$$n_{\max} \simeq 2\lambda/\varepsilon^2 \tag{14}$$

where ε is the relative accuracy required. Thus for $\varepsilon = 0.01$, which is the accuracy we used throughout this work, and $\lambda = 10$ we need as much as $n_{\max} = 2 \cdot 10^5$ iterations.

As noted by Johnston and Kunz [34], for such very long strips the variation of λ_n from step to step is very small due to averaging, and this can lead to a false impression of convergence. We wish to emphasise that we have used the quentity Δ_n^2 to determine when to break off the iterations, in spite of the (false) impression of wasting computer time calculating small changes in λ_n.

b) Transfer Matrix Method

Equation (3) can be rewritten in the form

$$\begin{pmatrix} A_{n+1} \\ A_n \end{pmatrix} = T_n \begin{pmatrix} A_n \\ A_{n-1} \end{pmatrix} \tag{15}$$

where T_n is the transfer matrix.

$$T_n = \begin{pmatrix} E - H_n & -1 \\ 1 & 0 \end{pmatrix}. \tag{16}$$

Given initial values for A_0 and A_1 the behaviour of A_n is given by

$$M_n = \prod_{\nu=1}^{n} T_\nu. \tag{17}$$

M_n satisfies Oseledec's theorem, namely that in the limit of large n the matrix $(M_n M_n^+)^{1/n}$ converges to a limiting matrix. This implies that the modulus of the eigenvalues of M_n and the corresponding eigenvectors are determined in this limit. In addition the product of T_ν acting on some vector will converge to the largest eigenvalue of M_n times its eigenvector. However, the required eigenvalue is that with modulus closest to unity, so that this procedure suffers from similar problems as the one discussed above, namely the tendency to lose the important eigenvalue due to rounding errors.

This can be overcome by the following transformation, which is carried out for each column B_i of the product matrix in succession (the index n is suppressed in these equations).

$$\bar{B}_i = (B_i - \sum_{j<i} (B_j \cdot B_i) B_j)/b^{(i)}, \tag{18a}$$

$$b^{(i)} = |B_i - \sum_{j<i} (B_j \cdot B_i) B_j|. \tag{18b}$$

Thus each column is orthonormalised to the previous ones. The first column converges to the eigenvector corresponding to the largest eigenvalue, the second column to the second largest and so on. As before it is unnecessary to perform this transformation after every stage of the calculation. In practice, since M_n and T_n are symplectic (i.e. eigenvalues occur in pairs, which are reciprocal of one another) it is only necessary to calculate half of them.

Again, as in the Green's function method the localisation length may be calculated by iteration. For a "bar" of cross section m

$$\lambda_n = \frac{n}{c_n^{(m)}} \tag{19}$$

where

$$c_n^{(m)} = \ln b_n^{(m)} + c_{n-1}^{(m)} \tag{20}$$

which may be compared with (10) and (11). The discussion on statistical errors in the previous section may equally be applied here. In particular (12) to (14) apply to each eigenvalue separately. Since we require that eigenvalue which gives the largest λ its error is also the dominant one.

c) Comparison of Methods

Both of the methods discussed have been used to study the localisation properties of quasi-one dimensional systems [36, 37, 40]. In general they yield the same raw results within the accuracy of the respective calculations. Apparent contradictions (Ref. 36 vs. Ref. 37) are due to differences in interpretation rather than in the raw results.

The matrices employed by the Green's function (GF) method are smaller than those required by the transfer matrix (TM) method. On the other hand the transformation required to preserve numerical stability is more complex in the GF case (7) than in the TM (18). The TM seems to be somewhat faster [40] although the exact comparison depends on such details of the implementation as the algorithm used for matrix inversion and the degree of parallelism of the machine used. The difference is small for the very large systems which dominate the total computer time.

The Green's function method is capable of generalisation to the calculation of more complicated properties of quasi-one dimensional systems [16, 41, 42]. The transfer matrix approach yields more information in that it gives all eigenvalues and eigenvectors, not just the dominant one. This has as yet not been used although the other eigenvalues may contain useful information [33, 34].

The GF approach is in principle sensitive to the initial conditions whereas the TM is not. In the systems considered here this is unimportant since the memory of the initial conditions is lost in a length comparable with the localisation length. This is not true in general however. Particularly in the presence of a magnetic field the initial conditions are important [43, 44].

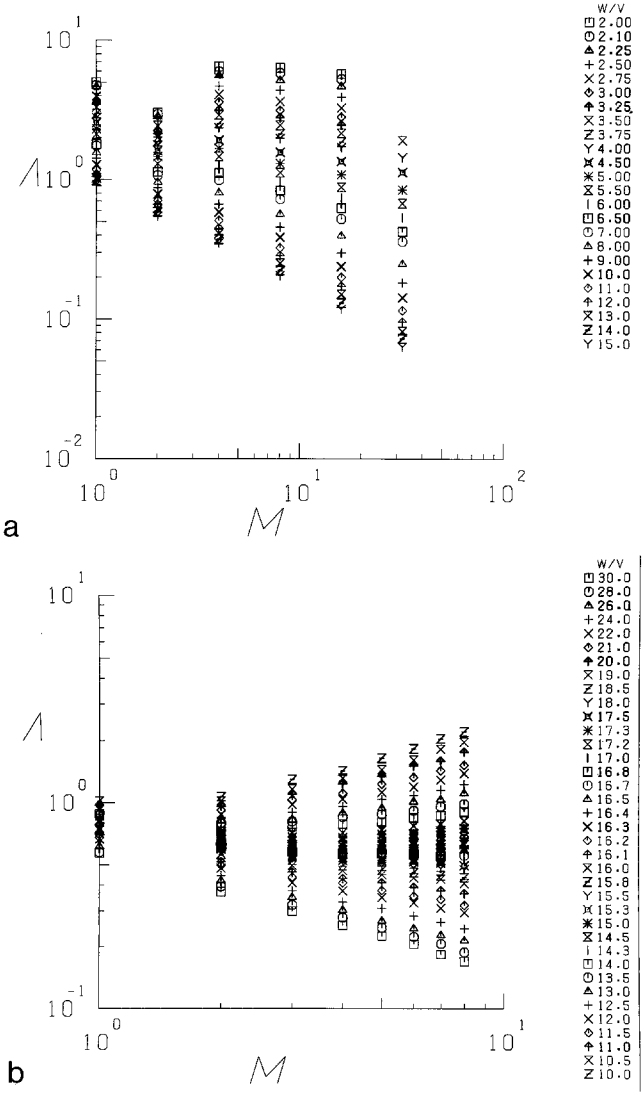

Fig. 1a and b. Double logarithmic plot of the renormalized exponential decay length $\Lambda = \lambda_M/M$ of the transmission coefficient of strips of width M **a** and bars of cross section $M \times M$ **b** as a function of M for the indicated values of the disorder parameter W/V

d) Results

The raw results of our calculations are plotted in Fig. 1 for strips and bars (i.e. $2d$ and $3d$ systems) for the center of the band, $E=0$. There is clearly a qualitative difference between the two cases. Whereas in $2d$, Fig. 1a, λ_M/M always falls with rising M. albeit weakly in some cases, in $3d$, Fig. 1b, there exists a value of $\lambda_M/M \approx 0.6$ above which λ_M/M rises with rising M.

This behaviour can be understood in a simple way as follows. λ_M/M falling implies that λ_M is tending to become small compared with M, so that the states will remain localised in an infinitely wide system. On the other hand λ_M/M rising implies that λ_M is tending to become large compared with M, so that the states are extended in an infinitely wide system. We thus have numerical confirmation that all states are exponentially localised in $2d$ as predicted by Abrahams et al. [1].

The remainder of the paper will be taken up by an extended analysis of these results and their implications for real systems.

3. Scaling Behaviour

a) General

The raw data shown above yield much more information when we analyse them by making use of the ideas of the renormalisation group [1, 20].

Let us define the renormalised localisation length on a "bar" as

$$\Lambda(M, W) = \lambda_M(W)/M \tag{21}$$

where W is a composite parameter representing disorder and energy. Thus Λ is simply the localisation length expressed in units of the strip width. The essential hypothesis of our analysis is that the behaviour of Λ under changes of length scale $M' \to bM$ depends on Λ alone, and not on M or W separately. This ansatz can be written as

$$\frac{d \ln \Lambda}{d \ln M} = \chi(\ln \Lambda). \tag{22}$$

This is equivalent to the condition that any change of length scale M can be compensated by a change in W so that the Hamiltonian remains essentially unchanged. Integrating (22) we obtain another useful form of the renormalisability condition

$$\Lambda(M, W) = f\{\xi(W)/M\} \tag{23}$$

where the constant of integration, $\xi(W)$, is a characteristic length which depends on W but not on M. The function f which is closely related to χ may depend on dimensionality and on certain symmetries but is otherwise universal [45–47].

Before applying these ideas to the analysis of our data let us consider the analytical properties of the scaling functions χ and f.

i) For small Λ the width, M, of the strip or bar is much larger than λ_M, so we expect λ_M to converge to its value for a $2d$ or $3d$ system. Thus

$$\chi(\ln \Lambda) = -1, \tag{24a}$$

$$\Lambda(M, W) = \xi(W)/M, \tag{24b}$$

$$f(x) = x. \tag{24c}$$

In this case we can identify the characteristic length $\xi(W)$ with the localisation length in the $2d$ or $3d$ system, $\lambda_\infty(W)$.

ii) For large Λ, λ_M is much larger than M and a wave travelling along the strip is evenly spread over the whole strip. The effective disorder seen by the wave in each slice of the strip is a statistical average over the disorder in the slice. The result of perturbation theory for $1d$ [48, 49] is also valid here, with the modified disorder:

$$W'^2 = W^2/M^{d-1}, \tag{25a}$$

$$\lambda_M \sim W'^{-2} = W^{-2} M^{d-1}. \tag{25b}$$

From these we can derive the behaviour of χ and f to be:

$$\chi(\ln \Lambda) = d-2, \tag{26a}$$

$$\Lambda(M, W) = (M/\xi(W))^{d-2}, \tag{26b}$$

$$f(x) = x^{2-d}. \tag{26c}$$

In this case $\xi(W)$ is related to the resistivity of the $3d$ system (see Sect. (4) below).

iii) From the behaviour of $\chi(\Lambda)$ near a fixed point, $\chi(\Lambda_c)=0$, we can calculate the critical indices [1]. Expanding χ around the fixed point gives

$$\frac{d \ln \Lambda}{d \ln M} = \chi' (\ln \Lambda - \ln \Lambda_c). \tag{27}$$

The solution of (27) can be written

$$\ln \Lambda = \ln \Lambda_c + [M/\xi(W)]^{\chi'} \tag{28}$$

where we have chosen the constant of integration to conform with (23) above. Since we expect Λ to be an analytic function of W for all *finite* M, $\xi(W)$ must be

chosen so that (28) has the form

$$\ln \Lambda = \ln \Lambda_c - A M^{\chi'}(W - W_c). \tag{29}$$

Comparing (28) and (29) we conclude that the critical index of ξ, ν, is equal to $-1/\chi'$ on both sides of the transition.

iv) For small disorder we can write down $\xi(W)$ by comparing (25) and (26) to obtain

$$\xi(W) \sim W^{2/(d-2)}. \tag{30}$$

The exponent $2/(d-2)$ in (29) suggests an essential singularity at $W=0$ for $d=2$ (see below). Our data for $\xi(W)$ fit

$$\xi(W) = (B/W^{\mu}) \exp(A/W^{\mu'}). \tag{31}$$

A and B being positive and μ, μ' of order unity.

b) Fitting Procedure

We shall now discuss the procedure used to test the data for scaling behaviour. Our analysis is based on a least squares procedure for fitting the parameters $\xi(W)$ in (23) above. If we plot our data in the form $\ln \Lambda(M, W)$ vs. $\ln M$ (as in Fig. 1) we have a set of curves characterised by different disorders, W. For most values of $\ln \Lambda$ there are several values of $\ln M$ corresponding to different W's. In order to conform with (23) the origin of $\ln M$ must be shifted to $\ln \xi(W)$ so that curves for different W overlap. A sufficient condition to achieve this is that the variance of the values of $\ln M - \ln \xi(W)$ corresponding to each value of $\ln \Lambda$ should be a minimum. This is achieved by minimising the quantity

$$S = \sum_i \left\{ \frac{1}{N_i} \sum_j [\ln M_{ij} - \ln \xi(W_j)]^2 - \left[\frac{1}{N_i} \sum_j (\ln M_{ij} - \ln \xi(W_j)) \right]^2 \right\} \tag{32}$$

where "i" is summed over Λ's and "j" over W's. $\ln M_{ij}$ is the value of $\ln M$ for a particular "i" and "j", obtained by simple linear interpolation (but not extrapolation) if necessary.

N_i is the number of curves at $\Lambda = \Lambda_i$. The minimum of S is obtained by solving the system of equations

$$\sum_j \left\{ \sum_i \left(\frac{1}{N_i^2} - \frac{\delta_{jk}}{N_i} \right) \right\} \ln \xi(W_j) = \sum_j \left\{ \sum_i \left(\frac{1}{N_i^2} - \frac{\delta_{jk}}{N_i} \right) \right\} \ln M_{ij}. \tag{33}$$

Unfortunately the matrix on the left of (33) is singular: it has at least one eigenvalue corresponding to a shift of the absolute origin of $\ln M - \ln \xi$, or of the mean corresponding to the variance in (32). It is therefore necessary to make an additional assumption about $\ln \xi(W)$. Equation (24) above tells us the behaviour for small Λ. By fitting the form

$$\Lambda = (a\,\xi/M) + b(a\,\xi/M)^2 \tag{34}$$

to the data for the largest disorder (i.e. smallest Λ's) it is possible to establish the absolute scale of $\xi(W)$. It should be noted that this procedure in no way changes the functional form of $\xi(W)$ but only its scale [50].

c) Discussion of the Scaling Curves

Figure 2 shows the results of our fitting procedure. In both $2d$ and $3d$ we have succeeded in putting all points with $M \geqq 4$ on one curve within the accuracy of the data, with the exception of those with $W = 2V$ in $2d$ (see Sect. 3e below). The curve for $2d$ (Fig. 2a) is qualitatively different from that for $3d$ (Fig. 2b). In $2d$ there is one branch and Λ always becomes very small for large M, whereas in $3d$ there are two branches the upper of which behaves like (26) for large M.

The presence of two branches is a sign of the existence of an Anderson transition. The inserts in Fig. 2 contain the calculated $\xi(W)$. The numbers are listed in Table 1. The function for $2d$ agrees with (31) for small W. However this form is rather insensitive to the precise values of μ and μ' for W within the range of our data. Setting $\mu = \mu'$ we obtain "best fit" values of $A = 12.5$, $B = 112$ and $\mu = \mu' = 1.5$, respectively. As is shown in Fig. 3a reasonable fits can also be obtained for μ between 1 and 2. It is perhaps worth noting that the value for $W = 2V$, $\xi \approx 10^6 a$ (a is the lattice constant) is a macroscopic length (≈ 1 mm) although W/V is still larger than unity and the disorder may not be considered a small perturbation of the ordered system. Such behaviour is characteristic of the critical dimensionality. Also worthy of note is that for $W = 6V$, $\xi \approx 10^2 a$. This length correponds to the maximum system size attainable with previous computational methods and corresponds therefore to the critical disorder predicted by them [51–54]. Indeed Yoshino and Okazaki gave an illustration of an extended state on a 100×100 square lattice at $W = 2V$ [51]. We now see that their lattice was four orders of magnitude too small to detect the localised nature of the state directly.

In $3d$ however we can extract little new information from $\xi(W)$. The critical disorder $W_c/V = 16.5 \pm 0.5$ agrees, more or less, with previous estimates [54]. It

Table 1. The scaling parameter $\xi(W)$ in units of the lattice distance a as function of the disorder parameter W/V for dimensions $d=2$ and $d=3$

$d=2$			$d=3$		
W/V	$\xi(W)/a$		W/V	$\xi(W)/a$	
2.00	0.7994	10^6	10.0	1.143	
2.10	0.3661	10^6	10.5	1.391	
2.25	0.1435	10^6	11.0	1.608	
2.50	0.3608	10^5	11.5	2.007	
2.75	0.1150	10^5	12.0	2.530	
3.00	0.5046	10^4	12.5	3.229	
3.25	0.2502	10^4	13.0	4.346	
3.50	0.1428	10^4	13.5	5.786	
3.75	0.7024	10^3	14.0	9.189	
4.00	0.4810	10^3	14.3	0.1170	10^2
4.50	0.1920	10^3	14.5	0.1437	10^2
5.00	0.9758	10^2	15.0	0.2204	10^2
5.50	0.5863	10^2	15.3	0.3086	10^2
6.00	0.3746	10^2	15.5	0.4444	10^2
6.50	0.2576	10^2	15.8	0.7119	10^2
7.00	0.1853	10^2	16.0	0.1062	10^3
8.00	0.1107	10^2	16.1	0.1292	10^3
9.00	7.296		16.2	0.1274	10^3
10.00	5.451		16.3	0.1379	10^3
11.00	4.220		16.4	0.1616	10^3
12.00	3.443		16.5	0.1690	10^3
13.00	2.915		16.7	0.1038	10^3
14.00	2.492		16.8	0.9304	10^2
15.00	2.200		17.0	0.7852	10^2
			17.2	0.5060	10^2
			17.3	0.4668	10^2
			17.5	0.3940	10^2
			18.0	0.2453	10^2
			18.5	0.1854	10^2
			19.0	0.1411	10^2
			20.0	8.502	
			21.0	6.370	
			22.0	4.992	
			24.0	3.457	
			26.0	2.596	
			28.0	2.212	
			30.0	1.867	

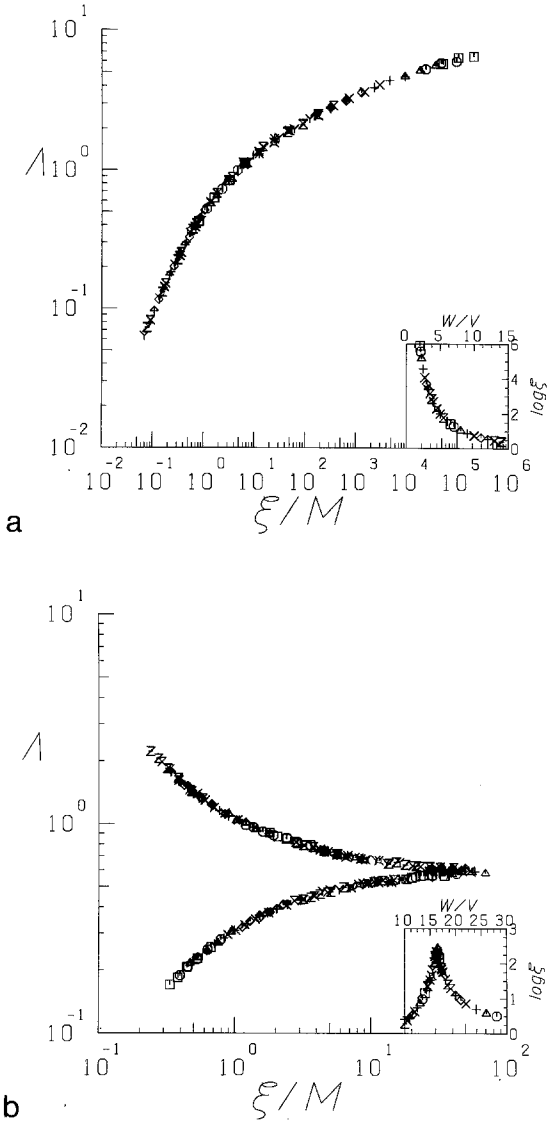

Fig. 2a and b. Double logarithmic plot of the renormalized decay length of the transmission coefficient Λ of strips of width M **a** and bars of cross section $M \times M$ **b** as a function of ξ/M. ξ is the scaling parameter, which is choosen to fit all data onto one and the same curve. The values of the disorder parameter W/V are the same as in Fig. 1. The inserts show the logarithm of the scaling parameter ξ, as a function of W/V

should be possible in principle to calculate the critical indices directly from $\xi(W)$ by plotting $\ln \xi$ vs. $\ln|W-W_c|$. Unfortunately the random errors in Λ tend to cause systematic errors in $\xi(W)$. To see why this is the case it is necessary to go back and re-examine our procedure for calculating $\xi(W)$. The error in $\ln \Lambda$ is independent of Λ and M. However, when the gradient of $\ln \Lambda$ vs. $\ln M$ is small, as it is near the fixed point, the procedure we have used tends to round off the singularity in $\xi(W)$. It is therefore necessary to ignore the immediate vicinity of $W = W_c$ and to estimate the critical indices from further away. By this method, although it seems to be somewhat contradictory, we estimate the critical indices to be equal and approximately equal to 1.2 ± 0.3. In the next section we shall discuss a more reliable method of estimating the critical indices.

Our calculated scaling curves, Fig. 2a, b are consistent with the predictions of (24) and (26) for large and small Λ. Earlier we suggested that in $2d$ the index $d-2$ in (26) might be indicative of logarithmic behaviour. To test this we have plotted Λ vs. $\ln(\xi/M)$ in Fig. 3b, and indeed obtained a straight line for large Λ (i.e. $\Lambda \gtrsim 2$). The gradient of this line was measured to be 0.63 ± 0.01 which is compatible with

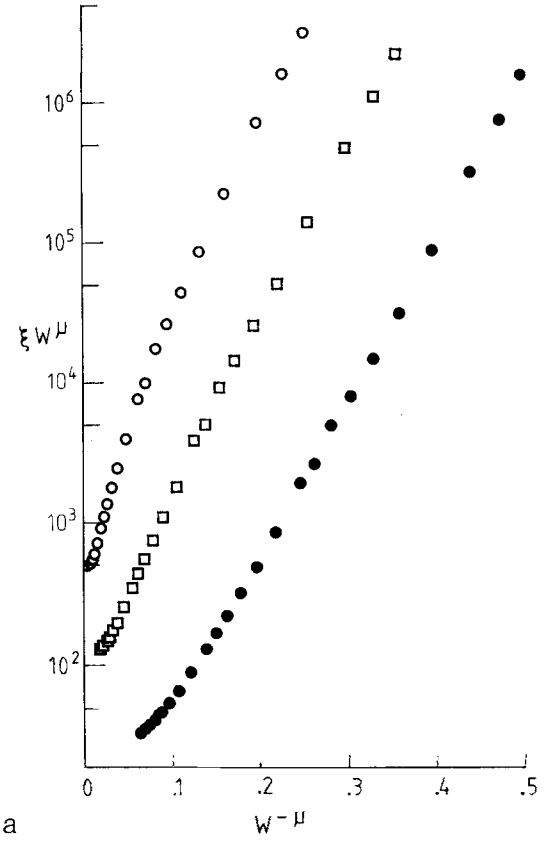

a

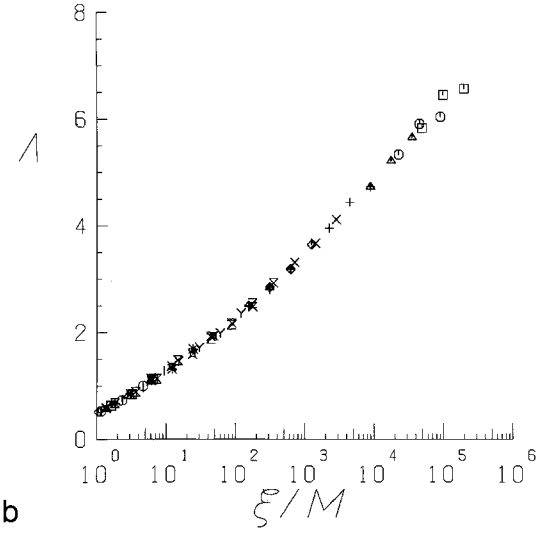

b

Fig. 3. **a** shows the logarithm of ξW^μ as a function of $W^{-\mu}$ for $\mu = 1$ (●), 1.5 (□) and 2 (○) for dimension $d=2$. The data are compatible with an essential singularily at $W=0$. **b** shows Λ as a function of the logarithm of ξ/M for dimension $d=2$. The curve becomes linear for large ξ/M thus demonstrating the logarithmic behaviour of (35)

$$\Lambda = \frac{2}{\pi} \ln[\xi(W)/M] \tag{35}$$

a form we shall require later.

d) Alternative Analysis

Although we could obtain considerable information from the above analysis the critical indices of the $3d$ system remain elusive. This was due to the singular behaviour of the scaling function at the fixed point which is difficult to reproduce numerically. In this section we present an analysis based on the ansatz (22). We expect this to be more reliable in the critical region since the function $\chi(\ln \Lambda)$ is analytic at $\chi = 0$. We first calculate the sums and differences of consecutive values of $\ln M$ and $\ln \Lambda$ for each value of W, from which we can write (22) in difference form

$$\frac{\Delta \ln \Lambda}{\Delta \ln M} = \chi(\overline{\ln \Lambda}). \tag{36}$$

In this form however the data are extremely noisy, due to the small value of $\Delta \ln M$ in the denominator. It is therefore necessary to smooth the data in order to proceed further. This can be achieved by fitting

$$\Delta \ln \Lambda_i = \{\chi_i + \chi_i'(\overline{\ln \Lambda} - \overline{\ln \Lambda_i}) + \chi_i''(\ln \Lambda - \ln \Lambda_i)^2\} \Delta \ln M_i \tag{37}$$

to the $\ln \Lambda$'s near each $\ln \Lambda_i \cdot \chi_i$ vs. $\ln \Lambda_i$ is then plotted in Fig. 4 for $2d$ and $3d$ (in $1d$ $\chi = -1$ for all Λ). One additional advantage of this procedure is that the validity of the scaling assumption can be tested by calculating

$$S^2 = \overline{(\Delta \ln \Lambda_i - \chi_i \Delta \ln M_i)^2}. \tag{38}$$

In $2d$ $S=0.01$ and in $3d$ $S=0.015$, which is about what would be expected from purely statistical factors, thus confirming our assumption of scaling. The $3d$ data fall more or less on a straight line of gradient

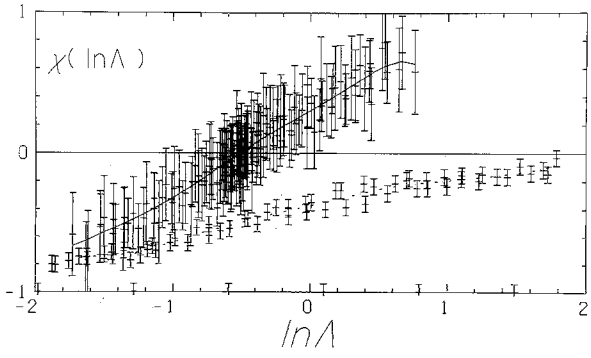

Fig. 4. Scaling function $\chi = d \ln \Lambda / d \ln M$ for the renormalized exponential decay length Λ of the transmission coefficient as a function of the logarithm of Λ for dimensions $d=2$ (lower data points with smaller error bars) and $d=3$ (upper data points with large error bars). For details of the calculation of the error bars see text. The curve represents the smoothed data (see text)

0.66 ± 0.02. This gives $\nu = 1.5 \pm 0.05$, which agrees with the estimate given by Sarker and Domany [22], contrasts however strongly with other estimates which mostly agree on $\nu = 1$ [20, 55, 56]. Such large difference between numerical and analytical results is somewhat surprising since the quantity S (Eq. (38)) confirms that the calculated systems are large enough for scaling to be valid. On the other hand the analytical estimates involve either expansions from large conductance (small disorder) or in $2+\varepsilon$ dimensions.

e) Deviations from Scaling

Although the results of the analysis in the previous sections seem to agree well with our scaling hypothesis, there are two important deviations from scaling behaviour, for small M and for small W. The simple form of (23) is only true when there are no other relevant lengths in the system comparable with ξ and M. For small M the lattice constant clearly becomes significant. The deviations from scaling seem to be greater for small disorder, however. A clue to this behaviour can be found by studying the dependence of Λ on the lateral boundary conditions [57, 58]. Figure 5 shows $\ln \Lambda$ vs. $\ln M$ for various W and with periodic and antiperiodic lateral boundary conditions. From this figure we see that the deviations from scaling are oscillatory and appear to change sign with change of boundary conditions. Thus the deviations from scaling behaviour are associated with the sensitivity of Λ to the lateral boundary conditions. In fact for free boundary conditions (not shown) the deviations are even larger, but this may be due to one dimensional surface effects.

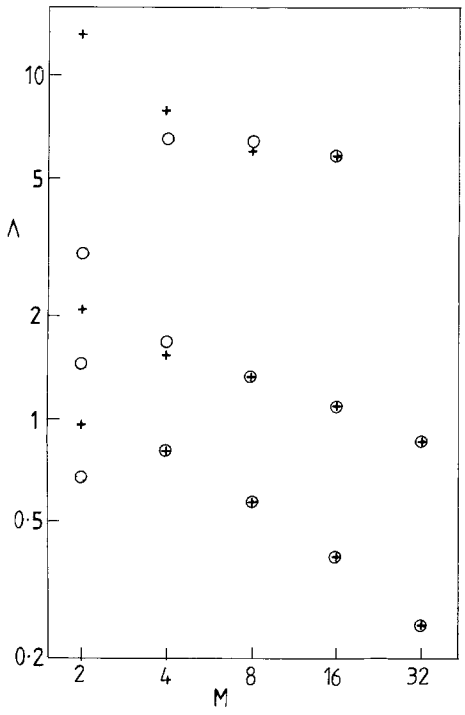

Fig. 5. The renormalized exponential decay length Λ of the transmission coefficient of strips as a function of the strip width M for periodic (○) and antiperiodic (+) boundary conditions across the strip. Upper, middle, and lower data points correspond to disorder parameters $W/V = 2, 5$, and 8 respectively

At first this may appear to be contradictory to the ideas of Thouless, who laid the groundwork for the scaling theory [59]. In that case, however, the sensitivity of the *energy levels* to boundary conditions gives a measure of the conductance. The sensitivity of the conductance and of such quantities as Λ to boundary conditions is a higher order effect. We would suspect such an effect to be related to the ratio of the phase correlation length, which may be related to the "mean free path" λ_{mfp}, to the strip width. This does not contradict Thouless since his ideas relate to diffusive transport. The mean free path however marks a transition from ballistic to diffusive behaviour (Ioffe-Regel criterion [60]) and thus presents a limit of scaling behaviour. This agrees well with the idea put forward by Wegner [45, 46] that local gauge invariance corresponding to $\lambda_{\mathrm{mfp}} \ll a$ is a prerequisite for scaling, and is implicitely assumed in many theories where $\lambda_{\mathrm{mfp}}^{-1}$ is introduced as the upper limit of an integral over reciprocal space.

In the thermodynamic limit this property, (namely local gauge invariance), is always fulfilled. In a real system, however, at finite temperature where the effective system size is determined by inelastic scattering the results of scaling will not necessarily apply if λ_{mfp} is longer than the inelastic scattering length. In that case the conductivity is due to ballistic transport between inelastic scattering processes and is purely Ohmic (see below Sect. 4b).

4. Transport Properties

a) Scaling of the Conductance

In order to compare the present theory with other scaling theories and with experiment we must establish a connection between Λ and some transport quantity. The theory of Abrahams et al. is expressed in terms of the dimensionless conductance $g = \frac{\hbar}{e^2} G$ and the β-function

$$\frac{d \ln g}{d \ln L} = \beta(g). \tag{39}$$

The function $\beta(g)$ has very similar properties to $\chi(\ln \Lambda)$, the most significant difference being that $\lim_{g\to 0} \beta(g) = \ln g$ whereas $\lim_{\Lambda\to 0} \chi(\ln \Lambda) = -1$. For these two quantities to be compatible it is sufficient that we can write, independent of the dimensionality,

$$g(L) = F[\Lambda(L)] \tag{40}$$

and we identify the length of a side of a square or cube, L, with the width of our strip or bar, M. In doing so we effectively consider a typical square or cube of size M^d cut from the strip or bar. We can now calculate the β-function from

$$\frac{d\ln g}{d\ln L} = \frac{d\ln g}{d\ln \Lambda}\frac{d\ln \Lambda}{d\ln M} = -\beta_1(g)\chi(\ln \Lambda) \tag{41}$$

where $\beta_1(g)$ is the β-function for a $1d$ system, where $\chi = -1$. Another way of reaching the same result is to consider the long strip or bar as made up of blocks of size M^d and Λ as the localisation length of the resultant $1d$ system of blocks. This is then a similar construction to the "block-spins" of the renormalisation group theory of phase transitions and contains all the relevant information for describing the critical behaviour. We are therefore justified in applying the Landauer [23] formula relating the conductance and the transmission coefficient of a $1d$ system to our system. Defining $T = \exp(-2/\Lambda)$, which is consistent with our original definition of λ_M, we can write [23, 24]

$$g = \frac{1}{\pi}\left(\frac{T}{1-T}\right) \tag{42}$$

from which we can derive

$$\beta_1(g) = (1+\pi g)\ln\left(\frac{\pi g}{1+\pi g}\right). \tag{43}$$

The β-functions calculated by this method are shown in Fig. 6.

By combining the above formula with (35) the form of β for large g regime of weak localisation in $2d$ is obtained as

$$\beta(g) = -\frac{1}{\pi^2 g} \tag{44a}$$

which is in agreement with most analytical expressions [1, 55]. Some apparent discrepancies of a factor of 2 are due to different counting of spins.

In $3d$ the data in Fig. 6 are consistent with

$$\beta(g) = 1 - \frac{a}{\pi^2 g} \tag{44b}$$

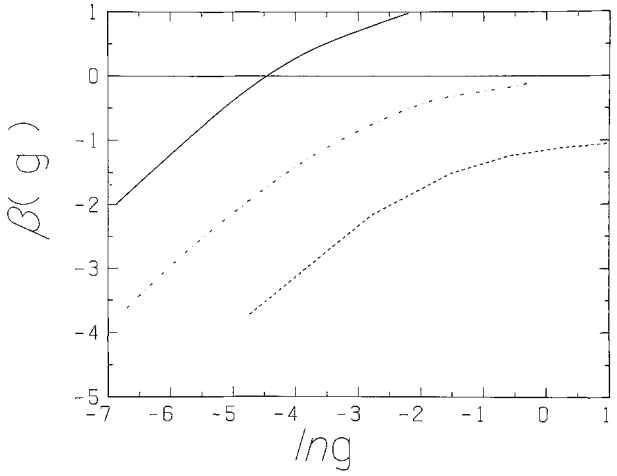

Fig. 6. Scaling function $\beta = d\ln g/d\ln M$ for the conductance g as a function of the logarithm of g for dimensions $d=1$ (dashed curve), $d=2$ (dashed-dotted curve) and $d=3$ (full curve)

where the constant a is of the order unity [61]. For very large g, where $\beta = 1$ we obtain

$$g = \sigma L. \tag{45}$$

Comparing this with (26) and (42) shows that

$$\xi(W) \sim \sigma^{-1}(W). \tag{46}$$

This identifies the characteristic length on the extended side of the transition with the resistivity.

At the fixed point $\beta = \chi = 0$ we have from (41)

$$\frac{d\beta}{d\ln g} = -\beta_1(\ln g)\frac{d\chi}{d\ln \Lambda}\cdot\frac{d\ln \Lambda}{d\ln g} = \frac{d\chi}{d\ln \Lambda} \tag{47}$$

so that the critical indices are the same in both cases, as expected.

Thus, under the assumption (40) the results presented here are fully compatible with the scaling theory of the conductance.

b) Temperature Dependence

Up to this point we have discussed our results purely in terms of the dependence of various properties on the size of the sample at $T = 0$ K. Such effects are extremely difficult, if not impossible to measure directly. It is much easier to measure the temperature dependence of the conductivity. How can we extract this information out of our results? The key idea to achieve this is that at finite temperature inelastic scattering processes play the dominant role in limiting the transport. The system is thought to be subdivided into subsystems of a diameter, which is giv-

en by the diffusion length L_i between two successive inelastic scattering events, and within which the transport may be thought as being determined only by the disorder [62–64]. The diffusion length is related to the inelastic scattering time τ_i via the diffusion constant D, i.e.

$$D\tau_i = L_i^2 \tag{48}$$

and replaces the system size L in the scaling equations. Since in the cases of interest the inelastic scattering time is related to the temperature by [64, 65]

$$\tau_i = A/T^p \tag{49}$$

where p is of the order of unity and A some constant, one can derive the temperature dependence of the conductivity from the scaling relations. This may be expected to work where the dependence is weak, as in thin metallic films, where the conductivity is larger ("weak localisation regime"). In more general cases it is not clear, however, whether such a procedure may be justified, because D itself becomes a function of the size of the system.

We first relate τ_i to the dimensionless conductance g via the Einstein relation.

$$\tau_i = \rho(E)\, L_i^d\, g^{-1} \tag{50}$$

where $\rho(E)$ is the density of states. Then we define a dimensionless conductivity by

$$\sigma' = g(L_i/\xi)^{2-d}. \tag{51}$$

Identifying L_i with M we may calculate this quantity from our data. Since $\rho(E)$ is only weakly dependent on L_i and g, and using (49) and (50), a plot of σ' versus $\ln g - d\ln M$ is essentially a plot of σ' against $p\ln T$ (Fig. 7).

The temperature dependence of the conductance and the conductivity may also be given in a diffential form, which may easily be derived from (50).

$$\frac{d\ln g}{d\ln \tau_i} = \beta(g)/(d-\beta(g)), \tag{52a}$$

$$\frac{d\ln \sigma}{d\ln \tau_i} = (\beta(g)-(d-2))/(d-\beta(g)). \tag{52b}$$

Using these relations we can discuss a number of limiting cases, which are of special interest with respect to recent experiments carried out on quasi-$2d$ metallic films and also on $3d$ systems.

(i) For small g, which implies large disorder, and/or very low temperature, such that

$$L_i(T) \gg \xi(W) > \lambda_{\mathrm{mfp}} \tag{53}$$

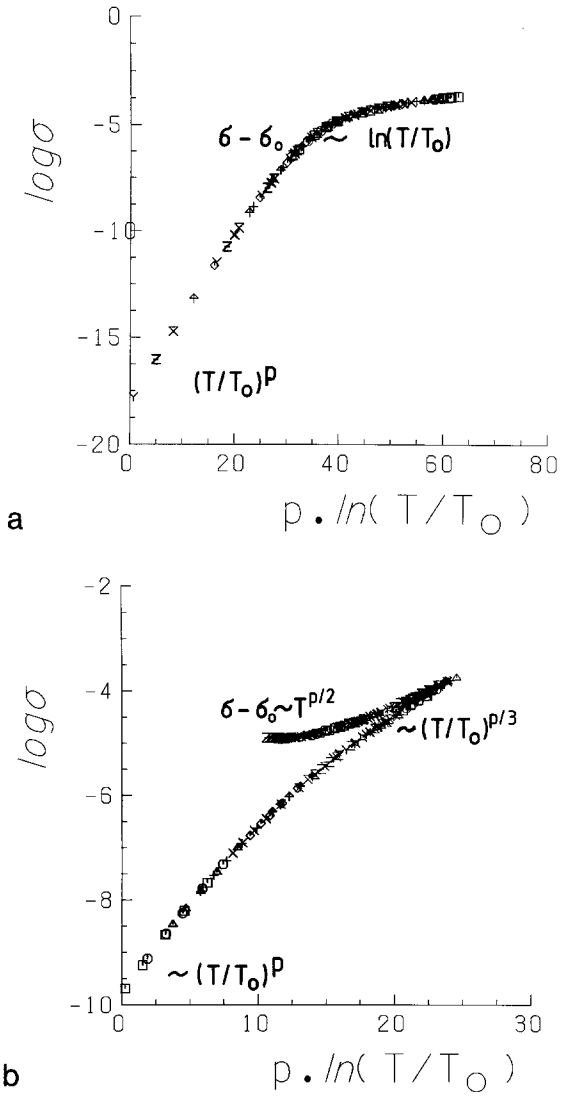

Fig. 7a and b. The logarithm of the dimensionless conductivity σ as defined in (51) as a function of $(\ln g - d\ln M)$ for dimensions $d=2$ **a** and $d=3$ **b**. As described in the text $(\ln g - d\ln M)$ is equivalent to $p\ln T/T_0$, where T is the absolute temperature, T_0 some suitable constant, and $p=0$ (1). The characteristic temperature regimes, which are described in the text (cf. (55), (58), and (61)), are indicated

Equation (52b) yields

$$\frac{d\ln \sigma}{d\ln \sigma_i} = -1 \tag{54}$$

since $|\beta(g)| \gg 1$.

Integration with respect to τ_i gives

$$\sigma = \sigma_0\, \tau_{i0}/\tau_i = \sigma_0 (T/T_0)^p \tag{55}$$

independent of the dimensionality. σ_0, τ_0 are integration constants. Thus a power law temperature de-

pendence appears as a consequence of the scaling theory rather than being in contradiction to it [66, 67]. According to (53) this is expected at very low temperatures.

ii) Increasing the temperature $L_i(T)$ decreases according to (48) and (49) and eventually

$$\xi(W) > L_i > \lambda_{\mathrm{mfp}}. \tag{56}$$

Near the Anderson transition in $3d$ where $\beta(g) \approx 0$ we have

$$\frac{d \ln \sigma}{d \ln \tau_i} = -\tfrac{1}{3}. \tag{57}$$

This gives by integration

$$\sigma = \sigma_0 (\tau_{i0}/\tau_i)^{1/3} = \sigma_0 (T/T_0)^{p/3}. \tag{58}$$

In the regime of "weak localisation" (cf. (44)) we have

$$\beta(g) = d - 2 - a/\pi^2 g \tag{59}$$

we obtain

$$\frac{d \ln \sigma}{d \ln \tau_i} = -\frac{1}{2\pi^2 \sigma} \quad (d=2), \tag{60a}$$

$$\frac{d \ln \sigma}{d \ln \tau_i} = -\frac{a}{2\pi^2} \left(\frac{\rho}{\sigma^3 \tau_i} \right)^{1/2} \quad (d=3). \tag{60b}$$

Integration yields

$$\sigma = \sigma_0 + \frac{p}{2\pi^2} \ln(T/T_0) \quad (d=2) \tag{61a}$$

and

$$\sigma = \sigma_0 + \frac{a}{2\pi^2} \left(\frac{T}{T_0} \right)^{p/2} \quad (d=3). \tag{61b}$$

Thus, the experimentally observed $\ln T$ behaviour of the conductivity in $2d$ appears also as a consequence of the scaling theory. It should be noted, however, that similar temperature dependences are also derived from interaction effects [8, 9, 68, 69]. In $3d$ the result (61b) has to be compared with earlier calculations in the weak scattering regime (68). Including electron-electron interactions yields a resistance increase as $T^{1/2}$ when T is decreased [68]. Assuming p to be of order unity, this is similar to the above result from the scaling theory, and seems to be in agreement with most recent measurements on metal semiconductor alloys [70].

iii) We expect the above temperature dependencies to be valid as long as relation (49) holds and $L_i > \lambda_{\mathrm{mfp}}$. For very high temperatures and/or low disorder this condition breaks down. We have classical Boltzmann like transport such that

$$\sigma \sim \tau_i \tag{62}$$

independent of dimensionality.

iv) For very low temperatures and localised states the inelastic scattering time τ_i is no longer independent of the transport process and we enter the hopping regime [71] where

$$\sigma \sim \exp\left[-\left(\frac{T_0}{T} \right)^{\frac{1}{(d+1)}} \right]. \tag{63}$$

5. Conclusions

We have presented numerical calculations of localisation for very long (up to 10^9 atoms) quasi one-dimensional systems. We were able to calculate the localisation length with an accuracy of 1% in all cases. The results are consistent with the assumption of scaling. From this it was possible to derive the critical properties of $2d$ and $3d$ disordered systems.

In $2d$ all states were found to be localised. The localisation length was however macroscopic for still fairly large disorder ($W = 2V$; $\lambda \approx 10^6$). In $3d$ there is an Anderson transition with critical indices $s = \nu \approx 3/2$. We have shown that deviations from scaling are related to the sensitivity to boundary conditions and that this happens when the system size is smaller than the phase correlation length or mean free path.

The relationship between the present theory and the scaling theory of the conductance is established and the influence of a finite temperature discussed. Apart from the well established results for high conductance (i.e. $\sigma = \mathrm{const} - \sim T^{p/2}$ in $3d$ and $\sigma \sim \ln T$ in $2d$) we have shown that for higher disorder or lower temperature the transport in localised states gives a power law $\sigma \sim T^p$ where p is the index in the dependence of inelastic scattering $\tau_i \sim T^{-p}$, an effect already observed by Davies and Pepper [66]. Near the mobility edge in $3d$ the conductivity obeys another power law, namely $\sigma \sim T^{p/3}$ in $3d$.

The method we have discussed here is capable of generalisation to a large number of related problems such as systems in a magnetic field and the quantised Hall effect, systems with spin orbit coupling or magnetic impurities [44] and to the study of finite size effects in microelectronic components.

This work was carried out at the Physikalisch-Technische Bundesanstalt, Braunschweig, at the University of Heidelberg and Imperial College, London using the TR 440 of the PTB, the IBM 370 of Heidelberg University, the CDC 7 600 of the University of Lon-

don and the Cray 1 of the SERC Daresbury Laboratory. Thanks are due to the members of the Solid State Theory Groups of the above institutions, to the staff of the respective computer centres, and to the participants of the Taniguchi symposium on Anderson Localisation, Japan 1981 and the DFG Symposium on localisation effects in $1d$ and $2d$ systems, Schleching, Germany, 1982. The work was supported by the German Federal Ministry of Economic Affairs and the British Petroleum Venture Research Unit.

References

1. Abrahams, E., Anderson, P.W., Licciardello, D.C., Ramakrishnan, T.V.: Phys. Rev. Lett. **42**, 673 (1979)
2. Gorkov, L.P., Larkin, A.I., Khmelnitzkii, D.E.: JETP Lett. **30**, 228 (1979)
3. Vollhardt, D., Wölfle, P.: Phys. Rev. B **22**, 4666 (1980)
4. Dolan, G.J., Osheroff, D.D.: Phys. Rev. Lett. **43**, 721 (1979)
5. Bishop, D.J., Tsui, D.C., Dynes, R.C.: Phys. Rev. Lett. **44**, 1153 (1980)
6. Dries, L. Van den, Haesendonck, C. Van, Bruynseraede, Y., Deutscher, G.: Phys. Rev. Lett. **46**, 565 (1981)
7. Markiewicz, R.S., Harris, L.A.: Phys. Rev. Lett. **46**, 1149 (1981)
8. Al'tshuler, B.L., Aronov, A.G., Lee, P.A.: Phys. Rev. Lett. **44**, 1288 (1980)
9. Al'tshuler, B.L., Khmelnitzkii, D.E., Larkin, A.I., Lee, P.A.: Phys. Rev. B **22**, 5142 (1980)
10. Yoshioka, D., Ono, Y., Fukuyama, H.: J. Phys. Soc. Jpn. **50**, 3419 (1981)
11. Al'tshuler, B.L., Aronov, A.G., Larkin, A.I., Khmelnitzkii, D.E.: Sov. Phys. JETP **54**, 411 (1981)
12. Dean, C.C., Pepper, M.: J. Phys. C **15**, L 1287 (1982)
13. Götze, W.: Modern problems in solid state physics. Lozovik, Yu.E., Maradudin, A.A. (eds.) Vol. 1. Amsterdam, Oxford, New York: North Holland (to be published)
14. Licciardello, D.C., Thouless, D.J.: J. Phys. C **8**, 4157 (1975); C **11**, 925 (1978)
15. Czycholl, G., Kramer, B.: Z. Phys. B - Condensed Matter **39**, 193 (1980)
16. MacKinnon, A.: J. Phys. C **13**, L 1031 (1980)
17. Thouless, D.J., Kirkpatrick, S.: J. Phys. C **14**, 235 (1981)
18. Czycholl, G., Kramer, B., MacKinnon, A.: Z. Phys. B - Condensed Matter **43**, 5 (1981)
19. Kramer, B., MacKinnon, A., Weaire, D.: Phys. Rev. B **23**, 6357 (1981)
20. Wegner, F.J.: Z. Phys. **25**, 327 (1976)
21. Lee, P.A.: Phys. Rev. Lett. **42**, 1492 (1979)
22. Sarker, S., Domany, E.: Phys. Rev. B **23**, 6018 (1981)
23. Landauer, R.: Philos. Mag. **21**, 863 (1970)
24. Anderson, P.W., Thouless, D.J., Abrahams, E., Fisher, D.S.: Phys. Rev. B **22**, 3519 (1980)
25. Stephen, M.J.: J. Stat. Phys. **25**, 663 (1981)
26. Erdös, P., Herndon, R.C.: Adv. Phys. **31**, 65 (1982)
27. Lee, P.A., Fisher, D.S.: Phys. Rev. Lett. **47**, 882 (1981)
28. Anderson, P.W.: Phys. Rev. **109**, 1492 (1958)
29. Hamer, C.J., Barber, M.N.: J. Phys. A **14**, 259 (1981)
30. Morgenstern, I., Binder, K., Hornreich, R.M.: Phys. Rev. B **23**, 287 (1981)
31. Nightingale, M.P.: Phys. Lett. **59** A, 486 (1977)
32. Sneddon, L., Stinchcombe, R.B.: J. Phys. C **12**, 3761 (1979)
33. Pendry, J.B.: J. Phys. C **15**, 3493, and 4821 (1982)
34. Johnston, R., Kunz, H.: Preprint J. Phys. C (to be published); Preprint J. Phys. C (to be published)
35. Weller, W., Prigodin, V.N., Firsov, Yu.A.: Phys. Status Solidi (b) **110**, 143 (1982)
36. MacKinnon, A., Kramer, B.: Phys. Rev. Lett. **47**, 1546 (1981)
37. Pichard, J.L., Sarma, G.: J. Phys. C **14**, L 127 and L 617 (1981)
38. Abrahams, E., Stephen, M.: J. Phys. C **13**, L 377 (1980)
39. Sak, J., Kramer, B.: Phys. Rev. **24**, 1761 (1981)
40. Soukoulis, C.M., Webman, I., Grest, G.S., Economou, E.N.: Phys. Rev. B **26**, 1838 (1982)
41. Graudenz, W.: Diplomarbeit (Universität Dortmund 1982)
42. Graudenz, W., MacKinnon, A., Kramer, B.: (unpublished)
43. MacKinnon, A., Kramer, B.: Application of high magnetic fields in semiconductor physics. In: Lecture Notes in Physics, Landwehr, G. (ed.), Vol. 177, p. 74 Berlin, Heidelberg, New York, Tokyo: Springer 1983
44. MacKinnon, A.: (unpublished)
45. Oppermann, R., Wegner, F.: Z. Phys. B - Condensed Matter **34**, 327 (1979)
46. Wegner, F.: Preprint Nr. 30, SFB 123. Universität Heidelberg 1979
47. Hikami, S.: Phys. Rev. B **24**, 2671 (1981)
48. Thouless, D.: In: III-Condensed Matter. Balian, R., Maynard, R., Toulouse, G. (eds.). Amsterdam, Oxford, New York: North-Holland 1979
49. Abrikosov, A.A., Ryzhkin, I.A.: Adv. Phys. **27**, 148 (1978)
50. This is a more sophisticated procedure than we used in our previous paper, so there are some numerical differences between the older results and those presented here.
51. Yoshino, S., Okazaki, M.: J. Phys. Soc. Jpn. **43**, 415 (1977)
52. Prelovsek, P.: Phys. Rev. B **18**, 3657 (1978)
53. Stein, J., Krey, U.: Z. Phys. B - Condensed Matter **37**, 13 (1980)
54. Weaire, D., Kramer, B.: J. Non-Cryst. Solids **35** & **36**, 9 (1980)
55. Vollhardt, D., Wölfle, P.: Phys. Rev. Lett. **48**, 699 (1982)
56. Prelovsek, P.: Phys. Rev. B **23**, 1304 (1981)
57. Haydock, R.: Phys. Rev. Lett. **49**, 694 (1982)
58. MacKinnon, A., Kramer, B.: Phys. Rev. Lett. **49**, 695 (1982)
59. Edwards, J.T., Thouless, D.J.: J. Phys. C **5**, 807 (1972)
60. Ioffe, A.F., Regel, A.R.: Prog. Semicond. **4**, 237 (1960)
61. Due to the computational limitations on the cross section of the bar in $3d$ we are not sure about the actual value of this constant.
62. Thouless, D.J.: Phys. Rev. Lett. **39**, 1167 (1977)
63. Anderson, P.W., Abrahams, E., Ramakrishnan, T.V.: Phys. Rev. Lett. **43**, 418 (1979)
64. Thouless, D.J.: Solid State Commun. **34**, 683 (1980)
65. Bergmann, G.: Z. Phys. B - Condensed Matter **48**, 5 (1982)
66. Davies, R.A., Pepper, M.: J. Phys. C **15**, L 371 (1982)
67. Mott, N.F., Kaveh, M.: J. Phys. C **14**, L 659 (1981)
68. Altshuler, B.L., Aronov, A.G.: Pis'ma Zh. Eksp. Teor. Fiz. **27**, 700 (1978); Solid State Commun. **30**, 115 (1979)
69. For a detailed review of interaction effects in the weakly localised regime see the excellent paper by H. Fukuyama, which is available as a technical report of ISSP, University of Tokyo, Ser. A No. 1904 (1983). In: Electron-electron interactions in disordered systems.
Pollak, M., Efros, A.L. (eds.). Amsterdam, Oxford, New York: North Holland (to be published)
70. Warnecke, P., Gey, U.: (unpublished)
71. Mott, N.F.: Philos. Mag. **19**, 835 (1969)

A. MacKinnon
The Blackett Laboratory
Imperial College
Prince Consort Road
London, SW 7 2BZ
England

B. Kramer
Physikalisch-Technische Bundesanstalt
Bundesallee 100
D-3300 Braunschweig
Federal Republic of Germany